Component Modularized Design of Musculoskeletal Humanoid Platform Musashi to Investigate Learning Control Systems

Kento Kawaharazuka[1], Shogo Makino[1], Kei Tsuzuki[1], Moritaka Onitsuka[1], Yuya Nagamatsu[1]
Koki Shinjo[1], Tasuku Makabe[1], Yuki Asano[1], Kei Okada[1], Koji Kawasaki[2] and Masayuki Inaba[1]

Abstract— To develop Musashi as a musculoskeletal humanoid platform to investigate learning control systems, we aimed for a body with flexible musculoskeletal structure, redundant sensors, and easily reconfigurable structure. For this purpose, we develop joint modules that can directly measure joint angles, muscle modules that can realize various muscle routes, and nonlinear elastic units with soft structures, etc. Next, we develop MusashiLarm, a musculoskeletal platform composed of only joint modules, muscle modules, generic bone frames, muscle wire units, and a few attachments. Finally, we develop Musashi, a musculoskeletal humanoid platform which extends MusashiLarm to the whole body design, and conduct several basic experiments and learning control experiments to verify the effectiveness of its concept.

I. INTRODUCTION

The tendon-driven musculoskeletal humanoid [1], [2], [3], [4], which imitates not only the human proportion but also the joint and muscle structure of human beings, has many benefits. For example, it can realize mechanical variable stiffness, measure muscle tensions by using not expensive torque sensors but pressure sensors or loadcells, apply ball joints that have no singularity, and use an underactuated system such as the spine. Also, its body, which has a muscle structure like the human body, is useful in the sense that we can understand the human body better, embed humanlike learning control systems, and realize more human-like motions.

In this study, we develop Musashi as a hardware platform to investigate learning control systems of musculoskeletal structures such as self-body image acquisition methods [5], [6] (Fig.1). We consider 3 requirements for such a musculoskeletal humanoid platform.

- It is a musculoskeletal humanoid with a flexible body structure.
- It has redundant sensors to investigate learning control systems.
- Its construction and reconstruction are easy, and we can transform the body structure.

To develop a musculoskeletal humanoid platform with such characteristics has 3 benefits.

- We can safely investigate learning control systems using the flexible body and variable stiffness control.
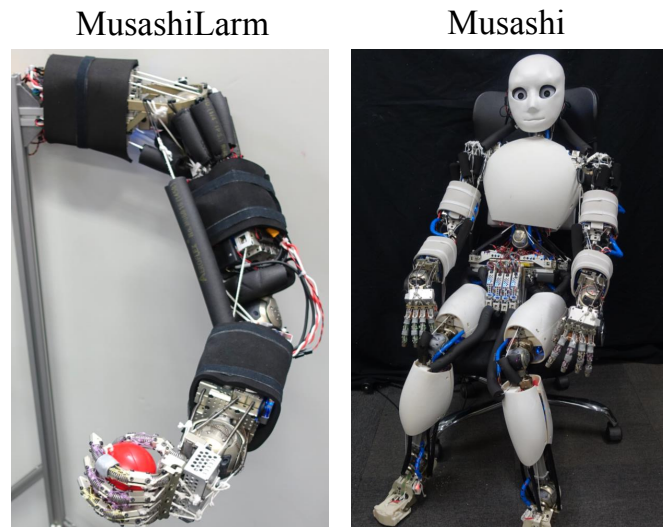
MusashiLarm   Musashi

Fig. 1: The newly developed MusashiLarm and Musashi.

- Although joint encoders usually cannot be installed in the musculoskeletal humanoid, a mechanism to directly measure joint angles makes experimental evaluations easy and accelerates developments.
- By changing link lengths, increasing degrees of freedom (DoFs), adding elastic elements, etc., we can consider changes in self-body image due to growth and deterioration of the body components.

To fulfill such requirements, we construct a new musculoskeletal humanoid Musashi using 3 concepts stated as below.

- A flexible body structure with nonlinear elastic elements having soft structures, and soft materials covering the folded back muscles.
- Joint modules which can directly measure joint angles and have compact sphere-shaped structures.
- A modularized body structure easily constructed using only joint modules, muscle modules, generic bone frames, muscle wire units, and a few attachments.

Musculoskeletal humanoids developed so far [1], [2], [3], [4] have very complex bodies mimicking the detailed human musculoskeletal structure at the cost of design effort. By component modularization, this study aims to accelerate the investigation of learning control systems by increasing flexiblity, redundancy of internal sensors, and easiness of design, at the cost of human-like ball joints and human-like body proportion to some degree.
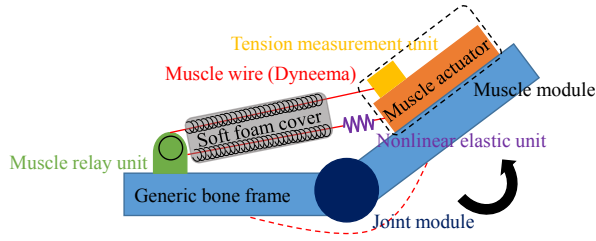
Fig. 2: Overview of the proposed musculoskeletal structure.

II. DEVELOPMENT OF RESPECTIVE MODULES

In this study, we propose the modularized musculoskeletal structure as shown in Fig.2. The joint module, which can directly measure joint angles, connects generic bone frames together, and the muscle module is attached to the bone frame. The muscle wire goes out from the tension measurement unit attached to the muscle actuator, is folded back through the muscle relay unit, and is attached to the nonlinear elastic unit. Also, the folded back wire in each muscle is covered by a soft foam cover. There is a spring between them in order to inhibit the friction between the wire and soft foam cover. This muscle configuration inhibits the decrease of transmission efficiency due to the use of a motor with a high gear ratio, and we expect it to have the same effect as planar muscles [7] by covering the entire joint with folded back muscle wires. Also, by adding the nonlinear elastic units and soft foam covers, we enable soft environmental contact and variable stiffness control.

In this study, we call the muscle components muscle wire unit, except for the muscle module. In the following sections, we will explain the detailed design of the joint modules, muscle modules, and muscle wire units.
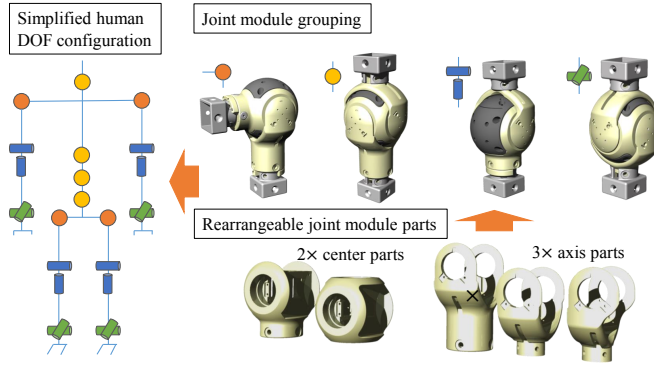

Fig. 3: Grouping of simplified human joints, and application of joint modules.

A. Joint Module

We set the requirements of the joint module, as below.
(1) It has a spherical shape for the muscles to be able to cover the joint like in human beings.
(2) It can measure joint angles in some way.
(3) Its circuits and cables are packaged compactly, and it can function as a stand-alone unit.

(4) It has a general versatility and can be used as any joint of the musculoskeletal humanoid.

Regarding (2), there are some methods to measure joint angles. In the ordinary axis-driven humanoid [8], each joint is independent, and each joint typically has an encoder or potentiometer. Also, there is a method to use an inertial measurement unit (IMU) to obtain joint angles from the acceleration and terrestrial magnetism. However, in the measurement of joint angles by IMU, we must use the terrestrial magnetism to inhibit the drift of yaw rotation, and so, it is difficult to measure joint angles correctly due to the noise of the many muscle motors included in the body of the musculoskeletal humanoid. Urata, et al. have developed a system to measure joint angles using a small camera [9], but we do not adopt it due to the system complexity. In this study, we design a sphere-shaped joint module which can directly measure joint angles using small potentiometers, like in the ordinary axis-driven humanoid. We compromise only on the point that it has a singularity like in the ordinary axis-driven humanoid.

Regarding (3), we package the circuits and cables that read potentiometers into this joint module compactly, and make it possible to function as a stand-alone, only by connecting a USB cable.

Regarding (4), the simplified human DoF configuration can be expressed as the left figure of Fig.3, if we ignore the complex scapula joint. We can group the joints into just 4 kinds of joint modules as shown in the upper right figure of Fig.3. We construct these 4 kinds of joint modules by combination of the 2 kinds of center parts and 3 kinds of axis parts, as shown in the lower right figure of Fig.3. By combining these 5 rearrangeable parts, we can construct various joint modules other than the 4 kinds of joint modules by adding or removing DoFs.
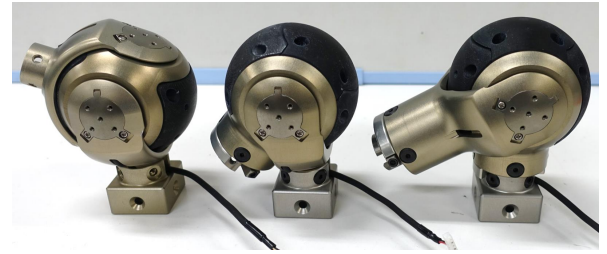

Fig. 4: Overview of the newly developed joint modules.

We show the developed joint modules in Fig.4. In order from the left, the joint modules are for the wrist, elbow, and shoulder joints.

The detailed structure of this joint module is shown in Fig.5. This is the structure of the shoulder joint module, and it is divided into 4 links, and 3 rotation axes exist among these links. Its structure is made by cutting A7075, and other parts are bearings, spacers, and circuit covers. A Potentiometer Board which reads the output of a potentiometer is arranged at each joint axis, and a Potentiometer Control Board which integrates them is arranged in the joint module. Also, its electrical wiring is shown in the right figure of Fig.5.
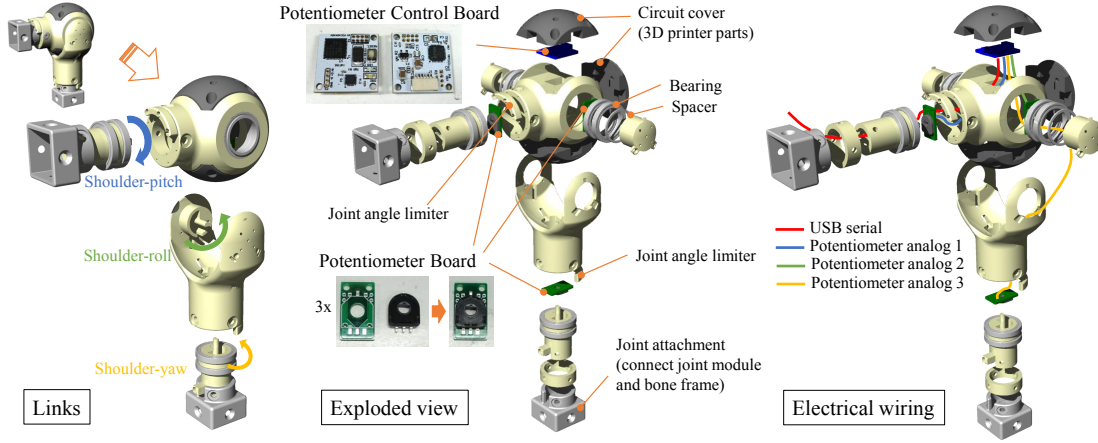
Fig. 5: Detailed design of the joint module, for the shoulder joint.

All of the electrical wiring that connects the Potentiometer Control Board and Potentiometer Boards passes through the joint module, except for one USB cable, which connects the joint module to the outside PC. The Potentiometer Control Board is equipped with IMU, which can be used for a more correct measurement of postures.

B. Muscle Module

First, we show the details of the sensor-driver integrated muscle module [10] in the left of Fig.6. This is the muscle module which dramatically increases the modularity and reliability by including $\phi22$ brushless DC motor, a pulley winding the muscle wire, motor driver, thermal sensor, tension measurement unit, circuit cover, etc. into one package. We can freely change the gear ratio of the actuator, but we used 29:1 or 53:1 in this study. The motor driver can conduct a current control and muscle tension control feedbacking muscle tension. We use chemical fiber Dyneema with high abrasion resistance as the muscle wires. The structure of the tension measurement unit is shown in the left of Fig.7, and this unit can measure muscle tension up to 500 N by converting it to the pressure to the loadcell using the angular moment around the axis. Also, as shown in the right of Fig.7, the tension measurement unit can be attached to the muscle actuator from various directions and realize various muscle routes.

Next, we show the details of the miniature bone-muscle module [11] in the right of Fig.6. A major difference of this module compared to the previous module is that this module can be used as not only the muscle actuator but also as the bone structure. This module includes 2 small $\phi16$ brushless DC motors. By including multiple actuators in one module, we can use space efficiently. "Base of bone" and "Support of bone" in Fig.6 become the body structure, and we can compactly construct the body structure with only muscle modules, by connecting these modules lengthwise and crosswise. Also, this module can compensate for the drawbacks adopting these small actuators, by dissipating the heat of the muscle actuator to "Base of bone" through "Heat-transfer-sheet".

These muscle modules are excellent in terms of the modularity, reliability, and versatility, so they can be the foundation of the musculoskeletal platform.
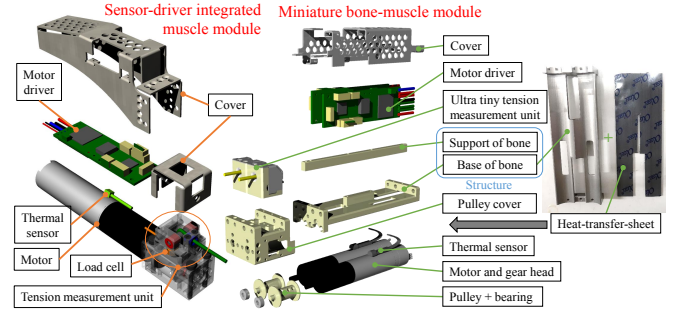

Fig. 6: Detailed design of the sensor-driver integrated muscle module [10] and miniature bone-muscle module [11].
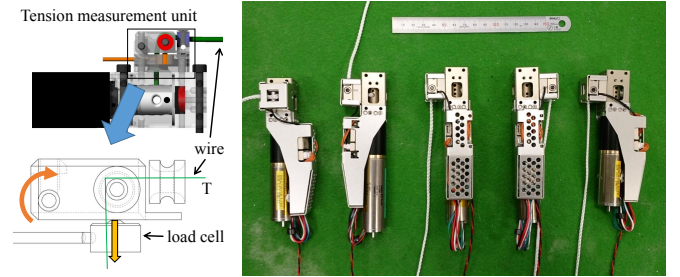

Fig. 7: The structure of the tension measurement unit, and the versatility of its arrangements to the muscle actuator.

C. Muscle Wire Unit

1) Muscle Relay Unit: We develop the muscle relay unit, which folds back a muscle wire, by arranging an axis with 3 bearings into a base structure. We can realize compact muscle relay units by directly using bearings to fold back muscles, without embedding the bearing into the structure. The structure of the muscle relay units can be standardized by the direction of attachment to the bone frame and the direction of the folded back muscle. We need to design only 3 kinds of muscle relay units shown in the upper figure of

Fig.8. We show the developed muscle relay units in the lower figure of Fig.8. This is the result of considering the most compact shape when setting the direction of the axis and the attachment by a screw. By choosing these units from the direction of the tapped holes and the direction the muscle will be folded back, we can quickly realize the muscle relay mechanism.
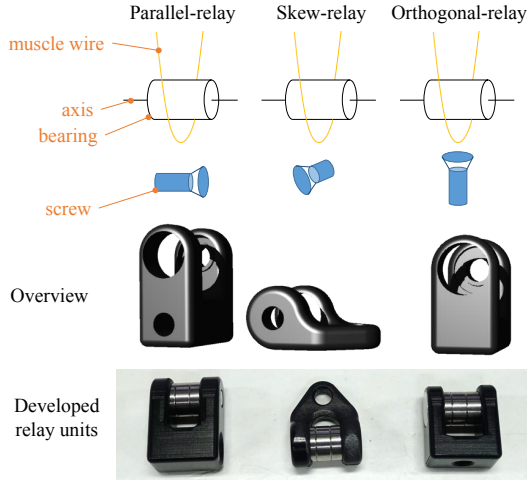

Fig. 8: Standardized 3 muscle relay units: Parallel-relay, Skew-relay, and Orthogonal-relay.

2) Nonlinear Elastic Unit: We show the previously developed nonlinear spring units in Fig.9. The two units in the left of Fig.9 are the nonlinear spring tensioner (NST) units for Kenzoh [12], and the right unit is the add-on nonlinear spring unit [13]. Although these units can geometrically realize nonlinear elasticity, they are too hard and large to use for the human-mimetic musculoskeletal structure because they are generally composed of metal and springs.

In this study, we develop a compact and flexible nonlinear elastic unit (NEU). The closest way to realize it is the method using O-ring, included in Anthrob [3]. However, the elastic unit in [3] could not express nonlinear elasticity.

We show the developed nonlinear elastic unit in Fig.10. The first unit is Oring-NEU. Although this is basically the same as the unit in Anthrob [3], only nitrile rubber could express nonlinear elasticity, when we tried some materials of O-ring (urethane, silicon, ethylene propylene, fluorine, and nitrile). However, nitrile rubber deteriorates by ozone in the air, and is easily ruptured from cracks. Also, because nonlinear elasticity can be obtained by pulling on the O-ring, there is a limit of muscle tension due to the strength of the rubber.

Then, we developed Grommet-NEU. The nonlinear elasticity can be expressed by compressing the grommet structure using the rolled muscle wire around it. In this structure, we can geometrically realize nonlinear elasticity, and so can freely choose its material. Also, the strength increases dramatically compared to Oring-NEU, because only the compression of the rubber is used. In this study, we use weather and water resistant ethylene propylene rubber as the grommet.
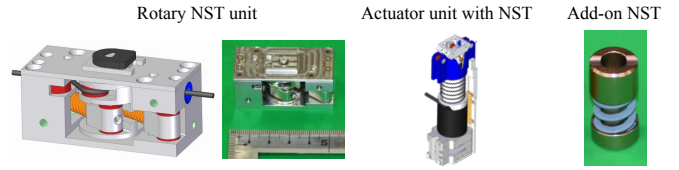

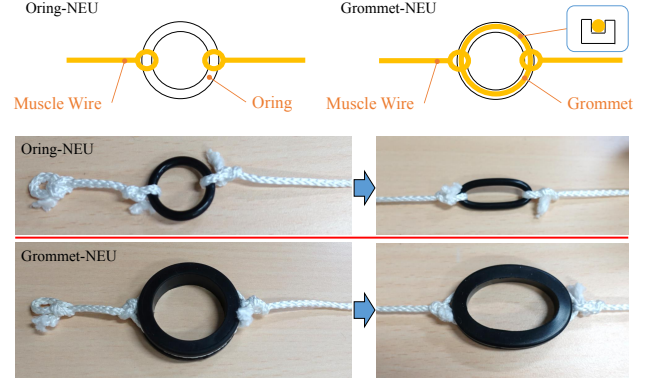Fig. 9: Previous nonlinear spring tensioner units [12], [13].

Fig. 10: Developed nonlinear elastic units: Oring-NEU and Grommet-NEU.

Finally, we conducted a parameter identification of this muscle configuration to verify the nonlinear elastic feature. The result is shown in Fig.11. As shown in the upper figure of Fig.11, we fix the absolute muscle length, wind the muscle wire, and identify the parameter by examining the amount of the wound muscle and the value of a force gauge. We assume that the relative change in muscle length is sufficiently small compared to the absolute muscle length. We show the result of the changes in muscle length and muscle tension in this condition, with the nonlinear elastic unit in the left figure, without the nonlinear elastic unit in the center figure, and with only the nonlinear elastic unit in the right figure of Fig.11. In this experiment, we fixed the absolute muscle length to 480 mm, and arranged the origin of the graphs by using the assumption that the elongation of the muscle is 0 when the muscle tension is 0. We can estimate the feature of the Dyneema as shown below, by using the assumption that its elongation is linear to the muscle tension and its spring constant is inversely proportional to the absolute muscle length, and executing least-square method (LSM):

$$T = a_d \Delta l_d / l_{abs} \tag{1}$$

where T [N] is the muscle tension obtained from the force gauge, a_d is the spring constant of Dyneema per unit length (in this study, a_d is estimated to be $2.8E+4$ from the lower center figure of Fig.11), Δl_d [mm] is the muscle elongation, and l_{abs} [mm] is the absolute muscle length. Also, we can estimate the parameters of this muscle configuration by LSM using an exponential function as shown below:

$$T = a_m \exp(b_m \Delta l_m) \tag{2}$$

where a_m, b_m are constants which express the nonlinear elastic feature (in this study, we estimated that $a_m = 1.34, b_m =$
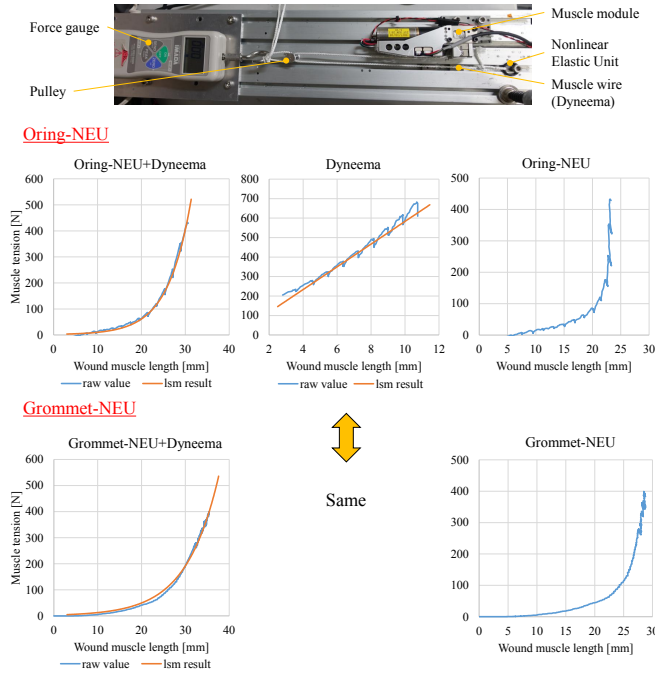
Fig. 11: Identification of nonlinear elastic parameters.

0.19 regarding Oring-NEU, and $a_m = 3.32, b_m = 0.14$ regarding Grommet-NEU, from the left figure of Fig.11). By using Eq. 1 and Eq. 2, the feature of the nonlinear elastic unit is expressed as shown below:

$$\Delta l_o = \Delta l_m - \Delta l_d = \frac{1}{b_m}\log(\frac{T}{a_m}+1) - \frac{T l_{base}}{a_d} \qquad (3)$$

where l_{base} is the absolute muscle length of 480 mm that is fixed in this study. So, by summing up the effects of Eq. 1 and Eq. 3, we can estimate the entire feature of this muscle configuration. T used in these equations is the output of the force gauge, and in actual use, we can measure half of T from the tension measurement unit, because each muscle is folded back through a pulley. Also, the muscle features of the actual robot may be different from the estimated features due to the effects of the soft foam cover, friction, etc., so the actual elastic feature needs to be learned by using the sensor information of the actual robot [6].

III. DESIGN OF MODULARIZED MUSCULOSKELETAL HUMANOIDS

A. MusashiLarm: Modularized Musculoskeletal Upper Limb

1) Body Structure: The detailed design of MusashiLarm is shown in Fig.12. MusashiLarm is composed of 4 links and 3 joints. We call these links the scapula, humerus, forearm and hand, respectively. The links of the scapula and humerus are constructed by aluminum generic bone frames, and in each link, 5 sensor-driver integrated muscle modules [10] are each connected to the generic bone frame through a muscle attachment. We can connect the muscle module to the generic bone frame, and the muscle modules to each other, through the muscle attachment. Also, the joint module and generic bone frame are connected through a joint attachment,

and if we change the joint attachment, we can change the configuration of the robot easily. The link of the forearm is composed of 4 miniature bone-muscle modules [11] which can connect lengthwise and crosswise as a bone structure. By using the benefit that the module can not only act as muscles but also as a bone structure, we do not need to use the bone frame, and the forearm link can easily be constructed using only the muscle modules. Also, the hand has flexible finger joints using machined springs [14].

In this way, we can realize easily constructable and reconstructable musculoskeletal body structures using joint modules, muscle modules, muscle wire units, generic bone frames, and a few attachments (muscle and joint attachments).
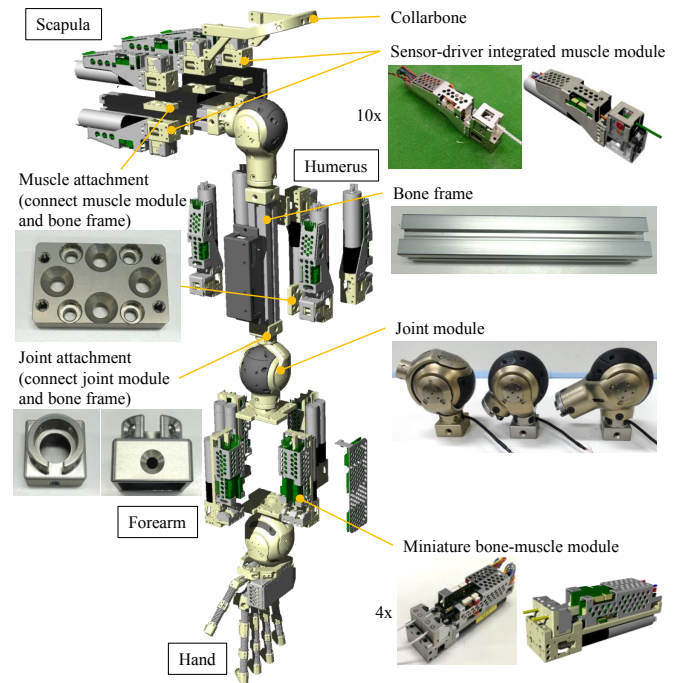

Fig. 12: Detailed modular design of MusashiLarm.

2) Muscle Configuration: The muscle arrangement of MusashiLarm is shown in Fig.13. The scapula and humerus include 5 muscles each, the forearm includes 4 miniature bone-muscle modules (8 muscles), and the total number of muscles is 18. These muscles imitate the basic muscles of the human body, and include polyarticular muscles. The nonlinear elastic units are applied to all muscles except for the ones moving the wrist and fingers, and we use brushless DC motors (90W, gear ratio is 29:1), as actuators.

3) Circuit Configuration: Next, the circuit configuration is shown in Fig.14, and we can connect new modularized components quickly in this configuration. The entire communication system is USB communication. Control Boards, a Loadcell Board, and Potentiometer Control Boards are connected to USB hubs which are arranged in the body. Control Boards are for the muscle motor control, a Loadcell Board amplifies the signal of loadcells attached to the hand
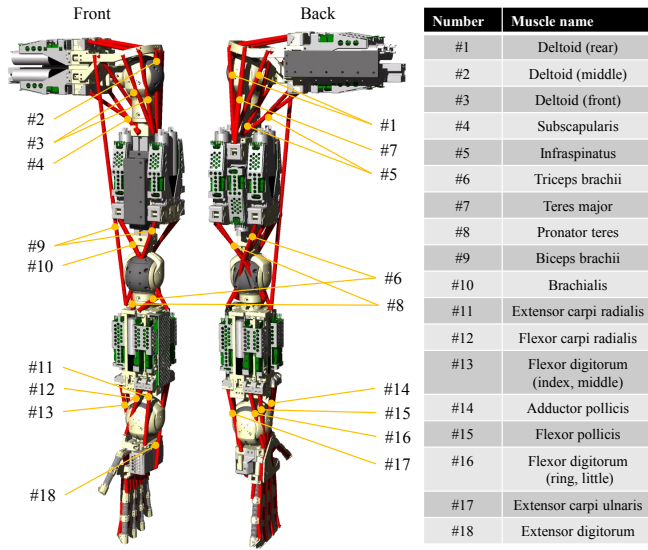
Fig. 13: Muscle arrangement of MusashiLarm.

Number	Muscle name
#1	Deltoid (rear)
#2	Deltoid (middle)
#3	Deltoid (front)
#4	Subscapularis
#5	Infraspinatus
#6	Triceps brachii
#7	Teres major
#8	Pronator teres
#9	Biceps brachii
#10	Brachialis
#11	Extensor carpi radialis
#12	Flexor carpi radialis
#13	Flexor digitorum (index, middle)
#14	Adductor pollicis
#15	Flexor pollicis
#16	Flexor digitorum (ring, little)
#17	Extensor carpi ulnaris
#18	Extensor digitorum

and integrates them, and Potentiometer Control Boards integrate the signal of potentiometers included in joint modules. Through the Control Board, motor drivers can connect up to 3 drivers by a daisy chain. Also, the Loadcell Board can read up to 12 signals of the loadcells, and the Potentiometer Control Board can read up to 4 signals of the potentiometers. The Potentiometer Control Board also sends the sensor information of the equipped IMU (MPU9250, InvenSense) to the PC (NUC, Intel), as redundant sensors.
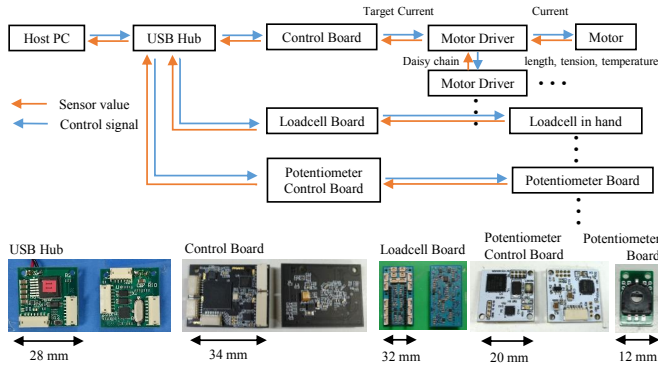

Fig. 14: Circuit configuration of MusashiLarm.

B. Musashi: Musculoskeletal Humanoid Platform

We can extend MusashiLarm with easily constructable and reconstructable structures to the whole-body musculoskeletal humanoid platform Musashi, by adding only a few joint attachments. As another example, this design has been applied to the two-wheel inverted musculoskeletal pendulum, TWIMP [15].

1) Body Structure: We show the musculoskeletal humanoid platform Musashi which extends MusashiLarm, in Fig.15. From the left, the figures are the overview, the body without muscle wires, the body without muscle wires and exteriors, and the body without muscle wires, exteriors, and muscle modules.

We basically extend the structure of MusashiLarm, but the muscle configuration in the lower limb is different from the upper. The gear ratio of the muscle actuators in the lower limb is 53:1, and there are no nonlinear elastic units and mechanisms folding back muscle wires.

Also, we show the body structure of only joint attachments, in the right figure of Fig.15. The number of additional joint attachments compared to MusashiLarm is 4, and so we use 5 kinds of joint attachments in Musashi in total. Thus, we can construct the whole body of Musashi using joint modules, muscle modules, muscle wire units, generic bone frames, and 6 attachments including the muscle attachment. As shown in the left figure of Fig.15, the upper legs, lower legs, chest, and head are covered with exteriors.
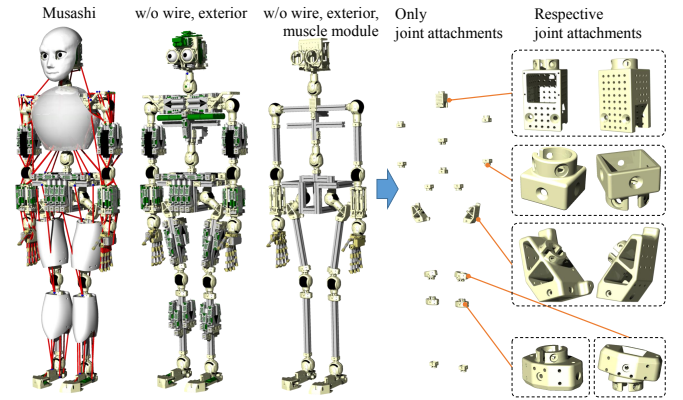

Fig. 15: Overview of Musashi body structure.

2) Head, Hand, and Foot: Although we stated the development of Musashi in terms of modularization, in this section, we introduce the characteristic structures of the head, hand, and foot of Musashi (Fig.16).

First, the head equips the movable eye-camera unit [16], and the camera has various functions such as resolution modification, auto focus, exposure compensation, etc. Musashi can recognize the self body by a wide perspective, measure the distance to an object by congestion, and change ROI, etc., and so we can accelerate learning control systems.

Second, the hand equips flexible and tough five fingers made of machined springs [14]. The thumb has a wide range of motion by a combination of machined springs, and the fingers have a variable stiffness mechanism. Also, the loadcells are equipped in the palm and fingertips, and we can use these sensors to detect environmental contact, as redundant sensors.

Third, the foot has a core-shell structure, which can measure contact force, in the toe and heel [17]. The structure can measure 6-axis force by the loadcells between the core and shell, and Musashi can measure force not only to the sole but also to the instep.

IV. EXPERIMENTS

A. Basic Experiments of MusashiLarm

First, we conducted a hammer hitting motion with a block. The result is shown in the center figure of Fig.17. Due to
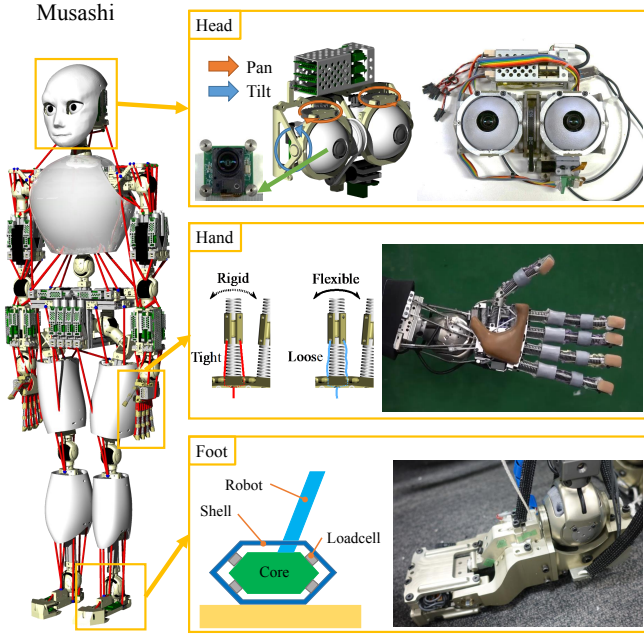
Fig. 16: Overview of Musashi head, hand, and foot.

the soft body, the upper limb can absorb external impact and parry force without breaking the robot itself.

Second, we conducted a dumbbell lifting motion with a dumbbell weight of 3.6 kg. The result is shown in the upper figure of Fig.17. Although the upper limb has a very soft body, it can exhibit high power and succeeded in lifting the dumbbell.
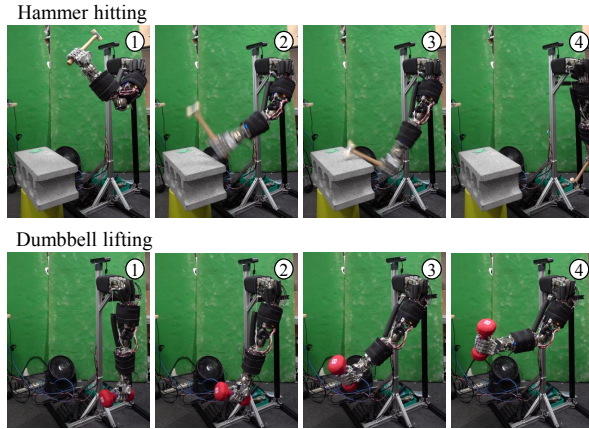

Fig. 17: Various motions using MusashiLarm.

B. Learning Control of Handle Operation

We conducted a handle operation experiment with Musashi, as an example of the environmental contact behavior by a flexible body using a learning control system. In the handle operation, the arm must move along the circular orbit and needs a large force. Also, we must accurately describe the relationship between the handle rotation and movement of the flexible arm.

Therefore, we use a learning control method [18] (Fig.18) which improved on the self-body image acquisition [6], and

the robot acquires handle operation while moving. We update the self-body image using the joint angles measured from the joint modules, and the muscle lengths and tensions measured from muscle modules. Then, we can conduct position control by calculating the target muscle length by inputting the target joint angles and measured muscle tensions into the self-body image. Musashi rotates the handle from -30 deg to 60 deg while solving inverse kinematics, and the self-body image is updated while moving. We can measure the rotation of the handle from AR marker. The experimental appearance is shown in the upper figure of Fig.19, and the transition of the handle rotation and muscle tensions is shown in the lower figure. In the beginning, the muscle tension is high at 270 N, and the handle rotates only about 40 deg in total. By updating the self-body image online, the relationship between joint angles, muscle lengths, and muscle tensions when rotating the handle, is learned. Finally, the handle rotates about 65 deg in total, and the maximum muscle tension to rotate it is about 180 N, because the difference between the actual robot and its geometric model including the antagonistic relationship is correctly modified. We were able to conduct an example of learning control systems using the redundant sensors and flexible structure of Musashi. However, it is difficult to completely conduct intended movements, and we would like to investigate learning controls considering hysteresis, etc., in the future.
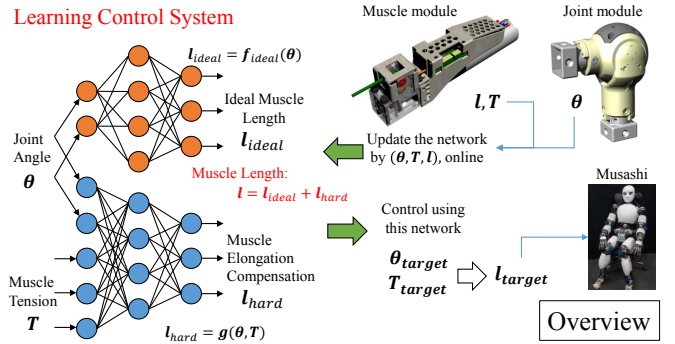

Fig. 18: The overview of the learning control system extending the previous method [6].

V. CONCLUSION

In this study, we stated the component modularized design of the musculoskeletal humanoid platform Musashi, to investigate learning control systems. At first, we set the flexible body, redundant sensors, and easily reconfigurable structure, as the requirements, and designed respective modules to fulfill them. We proposed generic joint modules including potentiometers and IMU, which can be applied to various joints and be used for redundant sensors in learning control systems. We designed 2 kinds of compact and reliable muscle modules, and used them depending on different body parts. Regarding muscle wire units, we standardized muscle relay units by the direction of the folded back muscle and the mounting direction, and realized compact and strong nonlinear elastic units with a soft structure, by
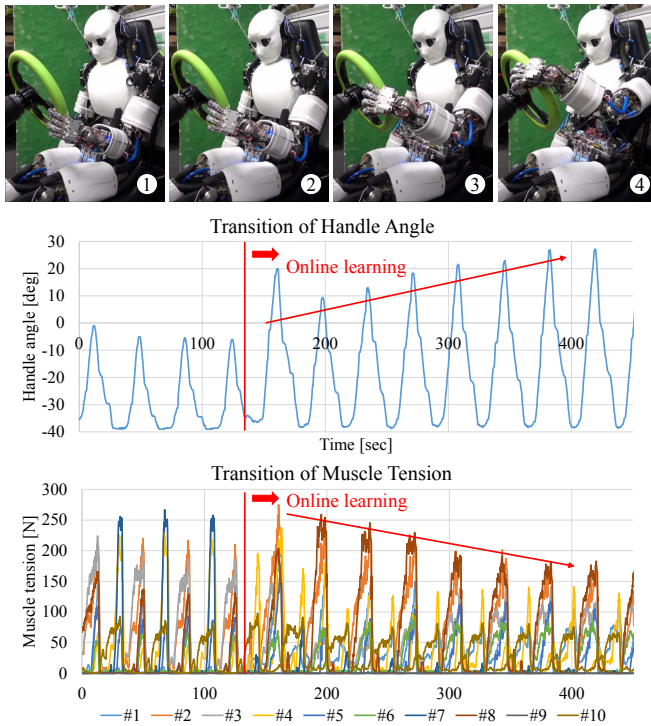
Fig. 19: The experiment of the handle operation. Lower graphs express the transition of the handle rotation angle and muscle tensions.

using the compression of the grommet structure. Then, we designed MusashiLarm composed of only joint modules, muscle modules, muscle wire units, generic bone frames, and a few attachments, and designed a musculoskeletal humanoid platform Musashi by extending MusashiLarm to the whole body with only 4 additional joint attachments. Also, we conducted experiments with environmental contact and using learning control systems, and verified the effectiveness of our concepts. In future works, we would like to investigate more advanced learning control systems using these musculoskeletal platforms.

REFERENCES

[1] Y. Nakanishi, S. Ohta, T. Shirai, Y. Asano, T. Kozuki, Y. Kakehashi, H. Mizoguchi, T. Kurotobi, Y. Motegi, K. Sasabuchi, J. Urata, K. Okada, I. Mizuuchi, and M. Inaba, "Design Approach of Biologically-Inspired Musculoskeletal Humanoids," *International Journal of Advanced Robotic Systems*, vol. 10, no. 4, pp. 216–228, 2013.

[2] S. Wittmeier, C. Alessandro, N. Bascarevic, K. Dalamagkidis, D. Devereux, A. Diamond, M. Jäntsch, K. Jovanovic, R. Knight, H. G. Marques, P. Milosavljevic, B. Mitra, B. Svetozarevic, V. Potkonjak, R. Pfeifer, A. Knoll, and O. Holland, "Toward Anthropomimetic Robotics: Development, Simulation, and Control of a Musculoskeletal Torso," *Artificial Life*, vol. 19, no. 1, pp. 171–193, 2013.

[3] M. Jäntsch, S. Wittmeier, K. Dalamagkidis, A. Panos, F. Volkart, and A. Knoll, "Anthrob - A Printed Anthropomimetic Robot," in *Proceedings of the 2013 IEEE-RAS International Conference on Humanoid Robots*, 2013, pp. 342–347.

[4] Y. Asano, T. Kozuki, S. Ookubo, M. Kawamura, S. Nakashima, T. Katayama, Y. Iori, H. Toshinori, K. Kawaharazuka, S. Makino, Y. Kakiuchi, K. Okada, and M. Inaba, "Human Mimetic Musculoskeletal Humanoid Kengoro toward Real World Physically Interactive Actions," in *Proceedings of the 2016 IEEE-RAS International Conference on Humanoid Robots*, 2016, pp. 876–883.

[5] K. Kawaharazuka, S. Makino, M. Kawamura, Y. Asano, K. Okada, and M. Inaba, "Online Learning of Joint-Muscle Mapping using Vision in Tendon-driven Musculoskeletal Humanoids," *IEEE Robotics and Automation Letters*, vol. 3, no. 2, pp. 772–779, 2018.

[6] K. Kawaharazuka, S. Makino, M. Kawamura, A. Fujii, Y. Asano, K. Okada, and M. Inaba, "Online Self-body Image Acquisition Considering Changes in Muscle Routes Caused by Softness of Body Tissue for Tendon-driven Musculoskeletal Humanoids," in *Proceedings of the 2018 IEEE/RSJ International Conference on Intelligent Robots and Systems*, 2018, pp. 1711–1717.

[7] M. Osada, T. Izawa, J. Urata, Y. Nakanishi, K. Okada, and M. Inaba, "Approach of "planar muscle" suitable for musculoskeletal humanoids, especially for their body trunk with spine having multiple vertebral," in *Proceedings of the 2011 IEEE-RAS International Conference on Humanoid Robots*, 2011, pp. 358–363.

[8] K. Kaneko, F. Kanehiro, S. Kajita, K. Yokoyama, K. Akachi, T. Kawasaki, S. Ota, and T. Isozumi, "Design of prototype humanoid robotics platform for HRP," in *Proceedings of the 2002 IEEE/RSJ International Conference on Intelligent Robots and Systems*, 2002, pp. 2431–2436.

[9] J. Urata, Y. Nakanishi, A. Miyadera, I. Mizuuchi, T. Yoshikai, and M. Inaba, "A Three-Dimensional Angle Sensor for a Spherical Joint Using a Micro Camera," in *Proceedings of the 2006 IEEE International Conference on Robotics and Automation*, 2006, pp. 4428–4430.

[10] Y. Asano, T. Kozuki, S. Ookubo, K. Kawasaki, T. Shirai, K. Kimura, K. Okada, and M. Inaba, "A Sensor-driver Integrated Muscle Module with High-tension Measurability and Flexibility for Tendon-driven Robots," in *Proceedings of the 2015 IEEE/RSJ International Conference on Intelligent Robots and Systems*, 2015, pp. 5960–5965.

[11] K. Kawaharazuka, S. Makino, M. Kawamura, Y. Asano, Y. Kakiuchi, K. Okada, and M. Inaba, "Human Mimetic Forearm Design with Radioulnar Joint using Miniature Bone-muscle Modules and its Applications," in *Proceedings of the 2017 IEEE/RSJ International Conference on Intelligent Robots and Systems*, 2017, pp. 4956–4962.

[12] Y. Nakanishi, T. Izawa, M. Osada, N. Ito, S. Ohta, J. Urata, and M. Inaba, "Development of Musculoskeletal Humanoid Kenzoh with Mechanical Compliance Changeable Tendons by Nonlinear Spring Unit," in *Proceedings of the 2011 IEEE International Conference on Robotics and Biomimetics*, 2011, pp. 2384–2389.

[13] M. Osada, N. Ito, Y. Nakanishi, and M. Inaba, "Realization of flexible motion by musculoskeletal humanoid "Kojiro" with add-on nonlinear spring units," in *Proceedings of the 2010 IEEE-RAS International Conference on Humanoid Robots*, 2010, pp. 174–179.

[14] S. Makino, K. Kawaharazuka, M. Kawamura, A. Fujii, T. Makabe, M. Onitsuka, Y. Asano, K. Okada, K. Kawasaki, and M. Inaba, "Five-Fingered Hand with Wide Range of Thumb Using Combination of Machined Springs and Variable Stiffness Joints," in *Proceedings of the 2018 IEEE/RSJ International Conference on Intelligent Robots and Systems*, 2018, pp. 4562–4567.

[15] K. Kawaharazuka, T. Makabe, S. Makino, K. Tsuzuki, Y. Nagamatsu, Y. Asano, T. Shirai, F. Sugai, K. Okada, K. Kawasaki, and M. Inaba, "TWIMP: Two-Wheel Inverted Musculoskeletal Pendulum as a Learning Control Platform in the Real World with Environmental Physical Contact," in *Proceedings of the 2018 IEEE-RAS International Conference on Humanoid Robots*, 2018, pp. 784–790.

[16] T. Makabe, K. Kawaharazuka, K. Tsuzuki, K. Wada, S. Makino, M. Kawamura, A. Fujii, M. Onitsuka, Y. Asano, K. Okada, K. Kawasaki, and M. Inaba, "Development of Movable Binocular High-Resolution Eye-Camera Unit for Humanoid and the Evaluation of Looking Around Fixation Control and Object Recognition," in *Proceedings of the 2018 IEEE-RAS International Conference on Humanoid Robots*, 2018, pp. 840–845.

[17] K. Shinjo, K. Kawaharazuka, Y. Asano, S. Nakashima, S. Makino, M. Onitsuka, K. Tsuzuki, K. Okada, K. Kawasaki, and M. Inaba, "Foot with a Core-shell Structural Six-axis Force Sensor for Pedal Depressing and Recovering from Foot Slipping during Pedal Pushing Toward Autonomous Driving by Humanoids (in press)," in *Proceedings of the 2019 IEEE/RSJ International Conference on Intelligent Robots and Systems*, 2019.

[18] K. Kawaharazuka, K. Tsuzuki, S. Makino, M. Onitsuka, Y. Asano, K. Okada, K. Kawasaki, and M. Inaba, "Long-time Self-body Image Acquisition and its Application to the Control of Musculoskeletal Structures," *IEEE Robotics and Automation Letters*, vol. 4, no. 3, pp. 2965–2972, 2019.